NASA/TM—1999-209281

IAF–98–J.2.01

Effects of G-Jitter on Directional Solidification of a Binary Alloy

C. Benjapiyaporn, V. Timchenko, G. de Vahl Davis, and E. Leonardi
Univeristy of New South Wales, Sydney NSW, Australia

H.C. de Groh III
Glenn Research Center, Cleveland, Ohio

Prepared for the
49th International Astronautical Congress
sponsored by the International Astronautical Federation
Melbourne, Australia, September 28—October 2, 1999

National Aeronautics and
Space Administration

Glenn Research Center

July 1999

Available from

NASA Center for Aerospace Information
7121 Standard Drive
Hanover, MD 21076
Price Code: A03

National Technical Information Service
5285 Port Royal Road
Springfield, VA 22100
Price Code: A03

EFFECTS OF G-JITTER ON DIRECTIONAL SOLIDIFICATION OF A BINARY ALLOY

C. Benjapiyaporn, V. Timchenko, G. de Vahl Davis and E. Leonardi
University of New South Wales, Sydney NSW, Australia

H C de Groh III
NASA Lewis Research Center, Cleveland OH, USA

Abstract A study of directional solidification of a weak binary alloy (specifically, Bi - 1 at% Sn) based on the fixed grid single domain approach is being undertaken. The enthalpy method is used to solve for the temperature field over the computational domain including both the solid and liquid phases; latent heat evolution is treated with the aid of an effective specific heat coefficient. A source term accounting for the release of solute into the liquid during solidification has been incorporated into the solute transport equation. The vorticity-stream function formulation is used to describe thermo-solutal convection in the liquid region.

In this paper* we present a numerical simulation of g-jitter. A background gravity of 1 μg has been assumed, and new results for the effects of periodic disturbances over a range of amplitudes and frequencies on solute field and segregation have been presented.

INTRODUCTION

The investigation of solidification and melting processes in low gravity conditions is of great practical importance for crystal growth techniques. The quality of single crystals grown from the melt strongly depends on growth morphology and macro-segregation in solidified ingots caused by convective heat and mass transfer effects. A low gravity environment produces conditions in which convection is decreased to a level at which crystal growth is largely diffusion controlled. Residual accelerations in orbiting space vehicles are of the order of one to several hundred μg (where 1 μg $=9.81\times10^{-6}$ ms^{-2}). For this reason, much effort has been expended in recent years in performing crystal growth experiments in the microgravity environment of a spacecraft in earth orbit. Such effects as compositional and kinetic supercooling, and the influence of convection on compositional distribution in the melt, have been investigated under microgravity.

However, gravity in an orbiting space vehicle may not be steady in either magnitude or direction. Perturbations to the anticipated steady microgravity environment may arise from, for example, crew actions, the operation of machinery and thruster rocket firings. Such perturbations are known as g-jitter.

The effects of gravity perturbations on composition distribution in Bridgman crystal growth configuration have been investigated numerically in a number of papers. Alexander, Ouazzani and Rosenberger[1] investigated the effects of steady and impulse residual acceleration on dopant distribution in Bridgman-Stockbarger crystal growth with different gravity vector orientations. It was found that lateral non-uniformity in composition is very sensitive to the orientation of the steady component of the residual gravity vector.

Transient and periodic accelerations have been considered in Alexander, Amiroudine, Ouazzani, and Rosenberger[2]. It was found that the largest compositional nonuniformities occur for disturbances with amplitudes above 10^{-6}g and frequencies below 10^{-2} Hz. At higher frequencies, larger acceleration amplitudes are required to obtain significant nonuniformities. Numerical results for the effect of g-jitter on the average interface concentration during Bridgman crystal growth in space are presented in Garandet, Corre, Favier and Alexander[3]. In all of these works a pseudo-steady-state model was adopted with the constraint that the interface is planar. This is a simplification of the true unsteady solidification process.

In actual growth situations the solid-liquid interface can be non-planar due to thermal and mass transfer conditions and also due to morphological instability factors. Pseudo-steady-state model neglects transient effects such as changes in the velocity, temperature and concentration with time due to changes in the length of melt caused by translating the ampoule. Investigation of solute redistribution during the initial transients becomes crucial for an alloy with a low partition coefficient solidifying at low rates because the steady state is difficult to reach in laboratory experiments.

In this work we investigate effects of periodic gravity perturbations on segregation and solute distribution during transient directional solidification of Bi-1%Sn alloy in a Bridgman furnace. A background gravity of 1 μg, which corresponds to a typical spacecraft environment, is considered.

MATHEMATICAL FORMULATION

We consider a Bridgman furnace in which a moving temperature profile consisting of a cold zone (T_c), a nominally adiabatic zone and a hot zone (T_h) is imposed on the boundary of the ampoule. This boundary temperature profile is translated with a constant pulling velocity as a result of the furnace movement causing the solid/liquid interface to move along the ampoule. The material in the ampoule is thus divided into two sub-regions: solid and liquid.

Although the ampoule is three-dimensional, a two-dimensional model is used. This simplification is valid because, under the microgravity conditions being considered, convection is very weak and the solidification process remains largely diffusion-controlled. Newtonian and laminar flow is assumed in the liquid phase, and the Boussinesq approximation has been used, in which the liquid density is assumed to be constant except in the buoyancy term of the equation of motion.

The governing time dependant equations describing mass, momentum, heat and solute transport in the vorticity-stream function formulation are:

$$\rho\left(\frac{\partial \zeta}{\partial t} + \nabla.\left(\tilde{V}\,\zeta\right)\right) = \nabla\rho \times \hat{g}\,|g| + \mu\nabla^2\zeta \qquad (1)$$

$$\nabla^2\psi = -\zeta \qquad (2)$$

$$\rho c_p\left(\frac{\partial T}{\partial t} + \nabla.\left(\tilde{V}\,T\right)\right) = \lambda\nabla^2 T \qquad (3)$$

$$\frac{\partial C}{\partial t} + \nabla.\left(\tilde{V}\,C\right) = D\nabla^2 C \qquad (4)$$

where t, ρ, μ, c_p, λ and D are respectively the time, density, viscosity, specific heat and thermal conductivity of the alloy and the diffusivity of the solute; ζ, ψ, T, $\tilde{V}$ and C are respectively the vorticity, stream function, temperature, velocity vector and solute concentration; g is the magnitude of the gravitational acceleration, and $\hat{g}$ is the unit vector in the direction of gravity. The density in the buoyancy term of equation (1) is assumed to be a linear function of temperature and solute concentration:

$$\rho = \rho_R\left[1 - \beta_T\,(T - T_R) + \beta_C\,(C - C_R)\right] \qquad (5)$$

where β_T and β_C are the thermal and solutal expansion coefficients,

$$\beta_T = -\frac{1}{\rho_R}\frac{\partial \rho}{\partial T} \qquad (6)$$

and

$$\beta_C = \frac{1}{\rho_R}\frac{\partial \rho}{\partial C} \qquad (7)$$

ρ_R is the reference density (the density of pure Bi at its melting temperature T_R) and C_R is the Sn concentration in pure Bi, namely zero.

The gravitational acceleration is taken as:

$$g(t) = g_0 + A\,\sin(2\pi\omega t) \qquad (8)$$

where A is the amplitude of the acceleration, ω is the frequency and g_0 is the steady component of the acceleration.

Enthalpy method

To model the process of directional solidification we have chosen the enthalpy method[4] which avoids explicit tracking of the solid/liquid interface.

Latent heat evolution during phase change is incorporated in the energy equation using the following definition of enthalpy. For each phase ϕ, enthalpy is defined as

$$h = \int_0^T c_{p_\phi}\,dT + f_l L, \qquad (9)$$

where L is latent heat and f_l is the local liquid volume fraction.

For isothermal phase change the liquid fraction is determined by the melting temperature T_m:

$$\begin{aligned} &\text{for } T > T_m \quad f_l = 1 \\ &\text{for } T < T_m \quad f_l = 0 \end{aligned} \tag{10}$$

With the assumption that specific heat $c_{p\phi}$ is constant in each phase, (9) can be written as

$$h = c_{p_\phi} T + f_l L = h_{sens} + f_l L\,, \tag{11}$$

Here h_{sens} is the sensible heat, and the subscripts l and s refer to the liquid and solid phases.

Using the apparent heat capacity method[5], an effective specific heat can be defined by

$$C^*(T) = \frac{\partial h}{\partial T} = c_{p_\phi} + L\frac{\partial f_l}{\partial T}\,. \tag{12}$$

Using (12), the energy equation (3) can be written:

$$\rho[C^*(T)\frac{\partial T}{\partial t} + c_{p_\phi}\nabla.(\tilde{V}T)] = \lambda\nabla^2 T\,. \tag{13}$$

To solve equation (13), an effective heat capacity coefficient $\partial f_l / \partial T$ has to be calculated. We define

$$\frac{\partial f_l}{\partial T} = \frac{\partial f_l / \partial n}{\partial T / \partial n} = \frac{(f_l)_n T_n}{T_n^2} = \frac{(f_l)_x T_x + (f_l)_y T_y}{T_x^2 + T_y^2} \tag{14}$$

where the subscripts n (denoting the normal direction), x and y denote differentiation.

Since isothermal phase change is under consideration, the liquid fraction undergoes a step change when the interface crosses a grid line. This abrupt change in the liquid fraction, defined by the step function (10), can cause serious numerical instabilities. To overcome this problem, a control volume was defined around each grid point, in which the liquid fraction could be estimated. Phase change was considered to take place over one control volume, in which the step function (10) is replaced by a linear approximation:

$$\begin{aligned} &\text{for } T_{i,j} > T_m + \Delta T && f_l = 1 \\ &\text{for } T_m - \Delta T \le T_{i,j} \le T_m + \Delta T && f_l = \frac{T_{i,j} - T_m + \Delta T}{2\Delta T} \\ &\text{for } T_{i,j} < T_m - \Delta T && f_l = 0 \end{aligned} \tag{15}$$

where $2\Delta T$ is a temperature interval chosen to represent the range over which phase change occurs in the (i, j) control volume.

Based on the calculated values of liquid fraction at each mesh point the computational domain was subdivided into sub-regions of solid and liquid phases. In the solid, the vorticity, stream function and velocities were set to zero. In the liquid, they are calculated from the stream function defined as:

$$\tilde{V} = \nabla \times \tilde{\psi} \tag{16}$$

Solute transport with phase change

The release of solute into the liquid during solidification can be described by considering an average concentration in an arbitrary control volume which is undergoing phase change (Voller, Brent and Prakash[4]). This control volume can be treated as partially solidified with an average concentration defined as:

$$C = f_s C_s + f_l C_l \tag{17}$$

where $f_s = 1 - f_l$ is the local solid volume fraction. Since diffusion in the solid is neglected, the concentration in the solid remains constant over time. Noting that $C_s = kC_l$ we can thus write:

$$\frac{\partial C}{\partial t} = -\frac{\partial f_s}{\partial t}(1-k)C_l + (1-f_s)\frac{\partial C_l}{\partial t} \tag{18}$$

When (18) is used in the solute transport equation (4), we obtain the solute conservation equation in the form:

$$\frac{\partial C_l}{\partial t} + \nabla.(\tilde{V}\,C_l) = D\,\nabla^2 C_l + S_c \tag{19}$$

in which

$$S_c = \frac{\partial f_s}{\partial t}(1-k)C_l + f_s\frac{\partial C_l}{\partial t} \tag{20}$$

The formulation for solute transport during phase change described by equations (19) and (20) allows for the solution for liquid concentration only and hence bypasses the concentration discontinuity at the interface.

NUMERICAL METHOD

An algorithm entitled SOLCON† [6], which incorporates the closely coupled solution of the transport equations

† SOLidification and CONvection

in the vorticity-stream function formulation, was used. To ensure stability of the computational process, all source terms and non-linear coefficients depending on liquid fraction are linearized based on the value of liquid fraction obtained from the previous iteration.

The vorticity, stream function and energy equations were discretized using central differences and solved by a modified ADI scheme with internal iterations. Interface boundary conditions for vorticity and stream function were applied at those mesh points in the solid sub-region which are adjacent to the liquid. For the calculation of vorticity boundary conditions, the definition of vorticity was used: $\tilde{\zeta} = \nabla \times \tilde{V}$. The boundary condition $\psi = 0$ was used for the stream function. The concentration equation (19) was discretized and solved using a control volume approach. This ensures mass balance during phase change in the partially solidified control volume. A second order upwind scheme (SOU) was used for the convection fluxes with central differences for the diffusion terms.

To account for the fact that the computed concentration is a cell average value, an exponential extrapolation procedure based on the liquid fraction has been introduced to find the values of the concentration at the solid/liquid interface. The liquid side interface solute concentration C_l can then be used to determine the concentration in the solid as it forms.

CODE VALIDATION

To validate the code computations were performed for directional solidification of gallium-doped germanium crystal grown by the Bridgman-Stockbarger technique as described by Alexander *et al.*[2]. Comparisons were made for the case of sinusoidal acceleration with an amplitude of 10^{-3}g and a frequency of 10^{-1} Hz oriented parallel to the solid-liquid interface.

In Alexander *et al.*[2] a pseudo-steady model was adopted with the assumption that the ampoule translation rate and the growth rate are equal. In their model the solid-liquid interface is located at a fixed distance from the top of computational domain, which is completely occupied by the melt. The aspect ratio of the computational domain was equal to 1. On the-other-hand the model used in the current study considers transient effects and hence the gradual decrease in the length of melting zone. Both solid and liquid phases are included in the computational domain (see Figure 1).

The temperature profile is translated with a constant pulling velocity along the boundary causing the interface movement inside the domain. The boundary temperature profile, size of the computational domain

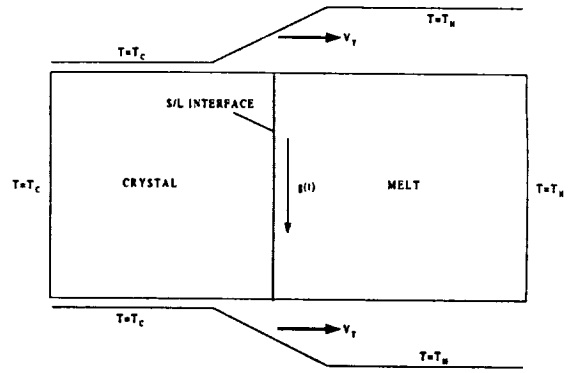

Figure 1. Model used in the present work for comparison with Alexander *et al.*[2]

and physical properties of the alloy were chosen to approximate the idealized model of the Bridgman-Stockbarger system in Alexander *et al.*[2]. T_c was equal to 1131K and T_h was 1331K. The length of the computational domain was taken to be 21 mm, the height was 10 mm and the adiabatic zone was 5 mm. A uniform square 51 x 106 mesh was used.

A steady solution for the temperature and flow was used as the initial condition for the transient growth. This steady solution was obtained by keeping the boundary temperature profile stationary with the solid-liquid interface located at 7 mm from the left wall of the ampoule. The initial solute concentration in the liquid was uniform at 1 at%. Solidification was first started with a constant gravity level of 1 μg and when 3 mm of material was solidified, a sinusoidal acceleration with an amplitude of 10^{-3}g and frequency of 10^{-1} Hz (oriented parallel to the solid-liquid interface) was imposed for another 2 mm of solidification. The translation velocity was 6.5 μm/s.

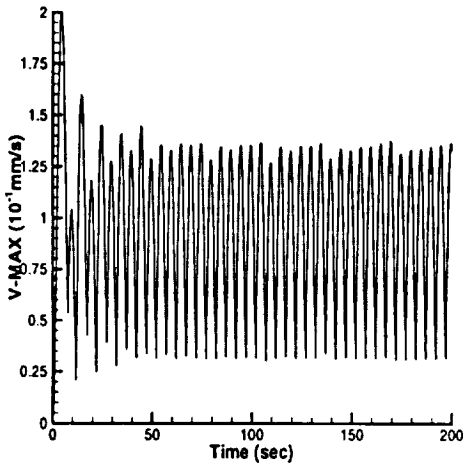

Figure 2. Maximum vertical velocity for a sinusoidal acceleration with an amplitude of 10^{-3}g and frequency of 10^{-1} Hz.

Figure 2 shows the maximum vertical velocity as a function of time computed using the present model. The velocity field is in phase with the residual acceleration. This result is in excellent agreement with Figure 7b from Alexander *et al.*[2].

Table 1. Comparison of the two models.

	U_{max} (mm/s)	V_{max} (mm/s)	$\gamma_{c\,max}-\gamma_0$ (%)
Alexander *et al.*[2]	0.1140	0.1325	19.14
Present work	0.1175	0.1338	19.80
% difference	3.07	0.98	3.5

Table 1 shows a quantitative comparison of the results obtained from the two models. U_{max} and V_{max} are the maximum horizontal and vertical components of velocity vector (during one period), and γ_c is the segregation defined by

$$\gamma_c = (C_{max} - C_{min})/C_{ave} \times 100\% \qquad (21)$$

where the three values of the concentration are taken at the interface and γ_0 is segregation before the g-jitter starts. In the case of Alexander *et al.*[2] γ_0 was equal to zero, in the present calculations the initial segregation was 4.0%.

The maximum change in segregation during g-jitter was equal to 19.14% (Alexander *et al.*[2]) and 19.8% (our calculations). This was reached after 230 seconds of solidification.

It is obvious that computed results are in very good agreement despite the difference in the physical and mathematical models.

SOLIDIFICATION OF BI-SN ALLOY

Simulations were performed for directional solidification of Bi-1at% Sn alloy in a Bridgman furnace. Property values are taken from Timchenko, Chen, de Vahl Davis and Leonardi[6].

The ampoule studied has a height of 6 mm and a length of 42 mm. The boundary temperature profile imposed on the liquid boundary consisted of a cold zone (T_c = 50 °C), linear temperature profile with a gradient 20 K/mm (for a length of 32.5 mm) and a hot zone (T_h = 700 °C). That is, conduction in the ampoule wall was not considered. The computational domain initially contains only liquid with a uniform solute concentration C_0 of 1 at% and uniform temperature of 700 °C. At the left boundary an initial temperature of 272 °C was imposed. The pulling velocity – the rate of translation of the boundary temperature distribution – was 3.34 μm/s, and solidification occurred from left to right as time progressed.

Mesh validation

To ensure the accuracy of the solution a mesh validation has been performed for 50 seconds of solidification. The amplitude of the gravity vector was taken to be 1 μg, acting in a direction normal to the axis of the ampoule.

Table 2. Mesh validation

	31 x 211	31 x 421	61 x 421
U_{max} mm/s	2.286×10^{-4} (0.7%)	2.286×10^{-4} (0.7%)	2.302×10^{-4} (–)
V_{max} mm/s	1.395×10^{-4} (0.35%)	1.400×10^{-4} (0.0%)	1.400×10^{-4} (–)

Three different mesh sizes were used, with the number of mesh points equal to 31 x 211, 31 x 421 and 61 x 421. The time step used with the 31 x 211 mesh was equal 0.1 s, and for the 31 x 421 and 61 x 421 meshes it was chosen equal 0.01 s. The difference between those results is listed in Table 2.

From Table 2, it can be concluded that a 31 x 211 mesh can be used in the calculations.

Solidification with g-jitter

The effects of periodic disturbances on the compositional profile and segregation at the interface have been investigated. The amplitudes were varied from 10^{-5}g to 10^{-2}g for a range of frequencies from 10^{-2} to 1 Hz.

At first, computations were performed for solidification with a constant gravity level of 1 μg. After 1500 seconds, sinusoidal accelerations oriented parallel to the solid-liquid interface were imposed and computations with g-jitter were performed for a further 500 seconds.

Table 3. Summary of results

Amplitude (m/s^2)	Frequency (Hz)	Maximum velocity (mm/s)		Maximum segregation (%)	Segregation at 500s (%)
		U_{max}	V_{max}		
10^{-2}g	0.01	2.50	0.89	188.7	90.0
	0.05	1.26	0.78	192.4	188.0
	0.1	0.75	0.32	39.9	39.9
	0.5	0.19	9.66×10^{-2}	20.2	20.2
	1.0	9.78×10^{-2}	4.81×10^{-2}	10.9	10.9
10^{-3}g	0.01	0.22	0.11	38.2	33.0
	0.05	0.12	6.75×10^{-2}	11.3	10.3
	0.1	7.49×10^{-2}	4.13×10^{-2}	8.9	8.9
	0.5	1.90×10^{-2}	9.78×10^{-3}	3.1	3.1
	1.0	9.95×10^{-3}	4.94×10^{-3}	2.5	2.5
10^{-4}g	0.01	2.15×10^{-2}	1.15×10^{-2}	4.9	4.3
	0.05	1.27×10^{-2}	6.86×10^{-3}	2.7	2.7
	0.1	7.68×10^{-3}	4.23×10^{-3}	2.3	2.3
	0.5	2.06×10^{-3}	1.08×10^{-3}	1.8	1.8
	1.0	1.14×10^{-3}	6.02×10^{-4}	1.8	1.8
10^{-5}g	0.01	2.41×10^{-3}	1.27×10^{-3}	2.0	2.0
	0.05	1.47×10^{-3}	7.96×10^{-4}	1.8	1.8
	0.1	9.66×10^{-4}	5.29×10^{-4}	1.8	1.8
	0.5	3.85×10^{-4}	2.12×10^{-4}	1.8	1.8
	1.0	2.97×10^{-4}	1.65×10^{-4}	1.8	1.8
	steady	2.28×10^{-4}	1.20×10^{-4}	1.8	1.8

For comparison purposes, computations with a steady gravity level of 1 μg were performed. The results of these computations are summarised in Table 3. It can be seen that for a given acceleration magnitude, larger segregation at the interface occurs for smaller frequencies or longer periods of disturbances. The same effect was reported in Alexander *et al.*[2]. Disturbances with amplitudes of 10^{-5}g produce very little effect on the segregation or the compositional profile. Disturbances with amplitudes of 10^{-4}g cause increases in the segregation between 2.7 to 4.9% (1.8% for steady 1μg gravity) when the frequencies of the disturbances become lower than 0.1 Hz. Larger effects on segregation were observed for disturbances with an amplitude of 10^{-3}g.

Figure 3 shows the vertical velocity at a reference point as a function of time, for frequencies of the disturbances of (a) 0.01 Hz, (b) 0.1 Hz and (c) 1 Hz with an amplitude of 10^{-3}g. The reference point is moving with the interface and is always located 2 mm in front of the interface at the mid-height of the ampoule. The development of the velocity field occurs in phase with the gravitational acceleration. The maximum velocity exhibits a transient before reaching steady oscillations. This transient includes number of periods which increases with increasing frequency as can be seen clearly in Figure 3(c). As the frequency is reduced the maximum velocity increases.

Figure 4 shows the velocity field for one cycle of the disturbance with an amplitude of 10^{-3}g and frequency of 0.01 Hz, starting from 300 seconds. During the first half of the cycle the gravity vector points downwards, with the maximum amplitude occurring at 325 seconds. Near the interface the predominant flow direction is also downwards. The velocity reaches a maximum at 330 seconds and then decreases as the magnitude of the gravitational acceleration decreases. At 350 seconds gravity reverses and as a result the velocity field also reverses, reaching the next maximum in about 380 seconds.

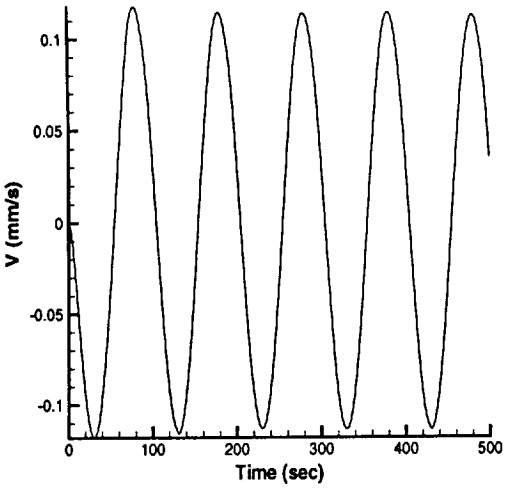

(a)

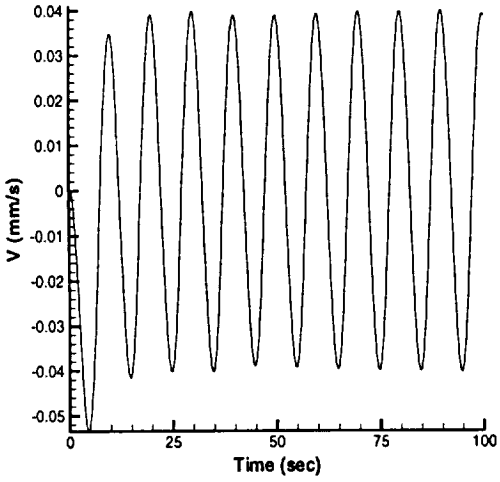

(b)

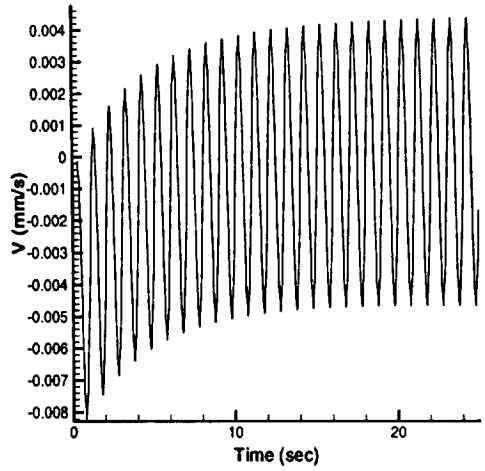

(c)

Figure 3. Vertical velocity at the reference point for an amplitude of 10^{-3}g and frequencies of (a) 10^{-2} Hz, (b) 10^{-1} Hz and (c) 1 Hz.

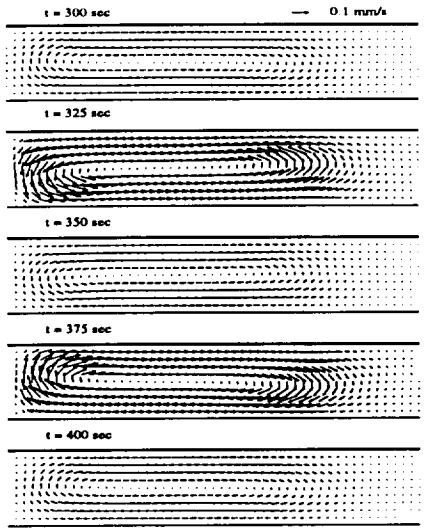

Figure 4. Velocity field: one cycle of the disturbance with an amplitude of 10^{-3}g and frequency of 0.01 Hz.

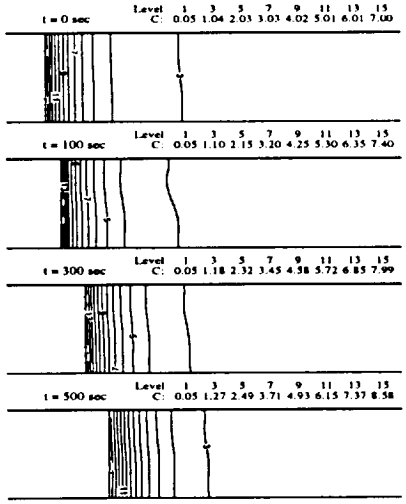

Figure 5. Solute field for the disturbance with an amplitude of 10^{-3}g and frequency of 0.1 Hz.

Concentration contours at 0, 100, 300 and 500 seconds after the start of g-jitter, with an amplitude of 10^{-3}g and frequencies of 0.1 and 0.01 Hz are shown in Figures 5 and 6 respectively. For a frequency of 0.1 Hz convection is weak and the concentration contours shown in Figure 5 have only slightly distorted. The segregation in this case increases from 1.8% to 8.9% by the end of 500 seconds of solidification. For 0.01 Hz the maximum segregation reaches 38.2% after 188 seconds of solidification and then decreases to 33% at the end of 500 seconds. In this case the flow carries low concentration solute from the bulk of the liquid to the interface and then redistributes it such that high concentration solute is located in the upper and lower parts of the interface. The concentration contours become much more distorted compared to the higher frequency case.

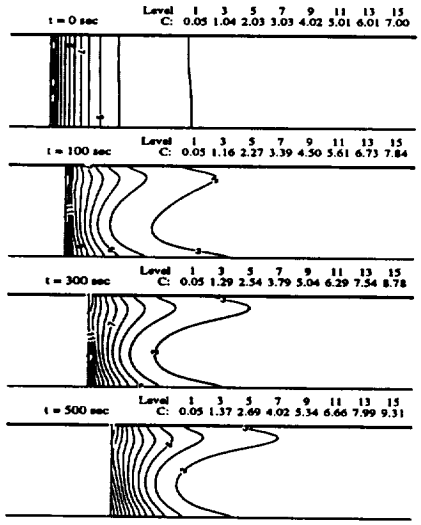

Figure 6. Solute field for the disturbance with an amplitude of 10^{-3}g and frequency of 0.01 Hz.

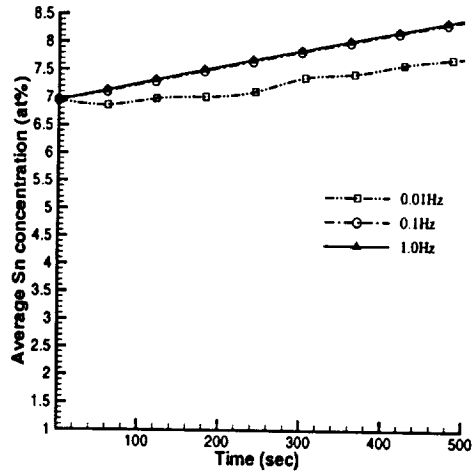

Figure 8. Average concentration at the interface for the disturbances with an amplitude of 10^{-3}g and frequencies of 10^{-2}, 10^{-1} and 1 Hz.

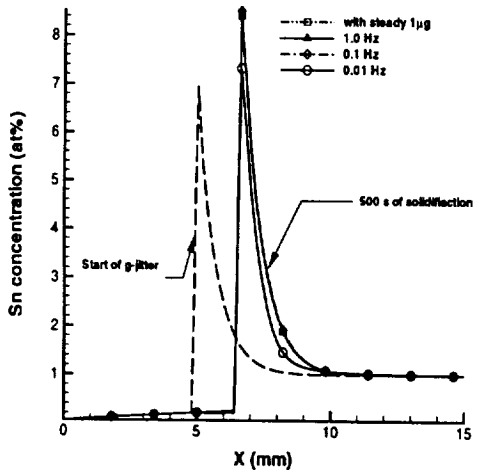

Figure 7. Distribution of solute concentration at the mid-height of the ampoule after 500 seconds of solidification.

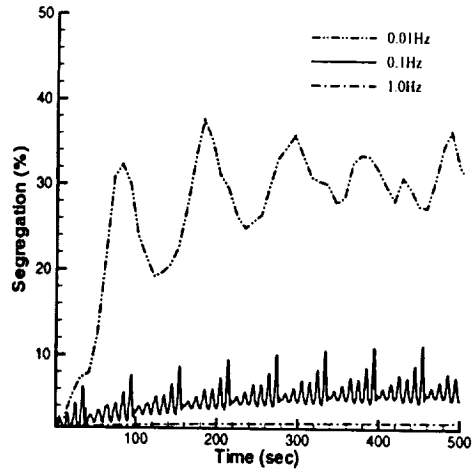

Figure 9. Segregation at the interface for the disturbances with an amplitude of 10^{-3}g and frequencies of 10^{-2}, 10^{-1} and 1 Hz.

Figure 7 shows the solute concentration distribution at the mid-height of the ampoule at the start of g-jitter and after a further 500 seconds of solidification for the three frequencies of 0.01, 0.1 and 1 Hz, for disturbances with an amplitude of 10^{-3}g and also for a steady gravitational acceleration.

By the time g-jitter starts the first 5 mm of the sample had been solidified, creating a solute rich boundary layer in front of the interface. This decays exponentially to C_0. The peak value of concentration at the interface caused by solute rejection into the liquid reached almost 7 at%.

After a the further 500 seconds of solidification the maximum concentration at the mid-height of the ampoule reached 8.33 at% for the steady gravitational acceleration, 8.43 at% and 8.38 at% for frequencies of 0.1 and 1Hz, and 7.26 at% for 0.01 Hz. The first three values only vary by 1.2% and correspond to diffusion-controlled plane front solidification. The largest difference in the maximum value (12.8%) occurs at the lowest frequency of 0.01 Hz. In this case convection has developed, resulting in the redistribution of solute in the melt and hence at the interface. The difference between the low 0.01 Hz frequency and the other cases can clearly be observed in Figure 8 which shows the history of the average

concentration at the interface during 500 seconds of solidification.

The resulting segregation at the interface can be seen in Figure 9. Clearly the segregation at the interface fluctuates with a frequency corresponding to that of the disturbances. For a frequency of 0.1 Hz, the segregation exhibits periodic oscillations after 200 seconds of g-jitter, whereas for a frequency of 0.01 Hz the periodic regime has not been reached by 500 seconds. The different magnitude of the peaks in the case of the 0.1 Hz frequency and their periodic change are not real but rather an artefact of the fixed grid finite volume formulation which is used. In this formulation all the computed values are cell averaged values which are changing while the interface passes through one partially solidified cell.

Finally, disturbances with an amplitude of 10^{-2}g are considered. This case exhibits not only quantitative change in the segregation for different frequencies but also different regimes of solidification. The time history of the average concentration at the interface during 500 seconds of solidification is shown in Figure 10. The response of the average at the interface concentration changes character with decreasing of frequency. At 1 Hz diffusion controlled growth is observed, with a gradual concentration increase due to release of solute in the liquid. Segregation is also increasing, reaching 10.9% after 500 seconds of solidification.

At 0.1 Hz the pattern is changing. The flow at first carries low concentration solute from the bulk of the liquid closer to the interface, some mixing occurs in the liquid and as a result the average concentration at the interface decreases while the interface is moving

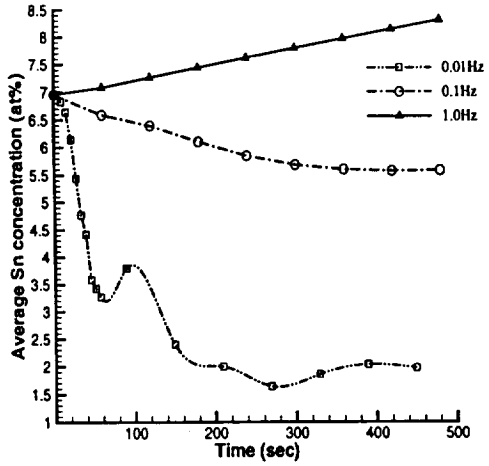

Figure 10. Average concentration at the interface for the disturbances with an amplitude of 10^{-2}g and frequencies of 10^{-2}, 10^{-1} and 1 Hz.

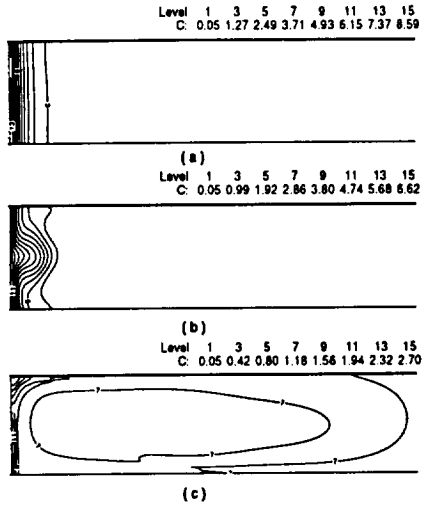

Figure 11. Solute concentration at 500 seconds for the disturbances with an amplitude of 10^{-2}g and frequency of (a) 1 Hz, (b) 0.1 Hz and (c) 0.01 Hz.

through the liquid. However, once the flow starts to oscillate backwards and forward, the average concentration reaches a steady state. The segregation in this case reaches 39.9% by 500 seconds. At 0.01 Hz the average concentration drops quickly due to mixing with solute from the bulk of the cavity. At 60 seconds the flow reverses and brings back high concentration solute causing an increase in the average concentration at the interface. As the magnitude of the velocity increases in the opposite direction, further mixing occurs in the liquid and the average concentration drops to 1.5%.

Figure 11 shows contours of concentration at 500 seconds for the disturbances with an amplitude of 10^{-2}g and frequency of (a) 1 Hz, (b) 0.1 Hz and (c) 0.01 Hz.

Figures 12 and 13 show the transformation of the flow structure from one configuration to another as a result of gravity reversal. These transitional stages are shown for 10^{-3}g in Figure 12 and for 10^{-2}g in Figure 13; the frequency of the disturbance was 0.01 Hz. Times shown are the 52^{nd} to 56^{th} seconds of a 100 second period. Gravitational vector reversal occurred at the 50^{th} second.

For 10^{-3}g (Figure 12), the flow goes through a transition from a counter clockwise main cell to the development of two small secondary and one stronger main cells and finally a single clockwise cell.

In the case of 10^{-2}g (Figure 13), distortion of the main flow cell has started after 30 seconds at which time the magnitude of the acceleration has started to decrease. The flow structure goes from a counter clockwise cell

structure to a flow with three secondary cells, then to a two cells structure and finally to the single cell flow structure at 57th second.

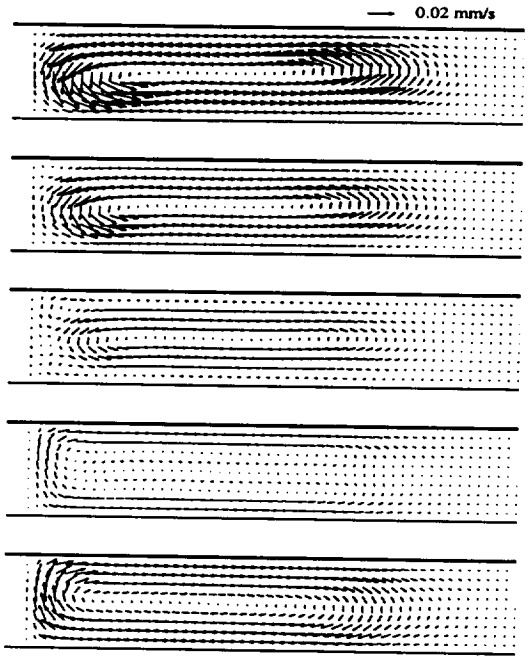

Figure 12. Flow reversal for the disturbance with an amplitude of 10^{-3}g and frequency of 0.01 Hz. Times from top to bottom are the 52nd to 56th seconds of a 100 second period.

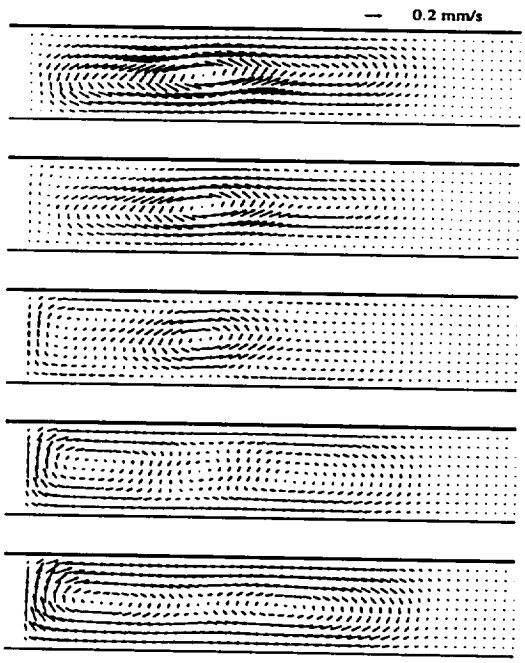

Figure 13. Flow reversal for the disturbance with an amplitude of 10^{-2}g and frequency of 0.01 Hz. Times from top to bottom are the 52nd to 56th seconds of a 100 second period.

CONCLUSIONS

We have investigated numerically effects of sinusoidal disturbances with amplitudes from 10^{-5}g to 10^{-2}g and frequencies from 10^{-2} to 1 Hz on the solute redistribution and segregation at the interface during directional solidification of Bi-1at% Sn alloy.

It was found that for large frequencies a higher amplitude of the gravitational acceleration is required to produce an effect on the segregation. For example, disturbances with frequencies from 0.5 to 1 Hz and amplitudes less then 10^{-2}g produce very little effect on the segregation. For this frequency range an amplitude of 10^{-2}g resulted in 20.2% and 10.9% segregation compared with a segregation of 1.8% for the steady 1 μg case. For frequencies from 0.05 Hz to 0.1 Hz, an amplitude of 10^{-3}g results in the segregation changing to 11.3% and 8.9% respectively. The largest effect on the segregation was produced by disturbances with a frequency of 0.01 Hz, where the maximum segregation was equal to 4.9% for an amplitude of 10^{-4}g, 38.2% for an amplitude of 10^{-3}g and 188.7% for an amplitude of 10^{-2}g. In the last case complete mixing of the solute in the cavity was observed.

REFERENCES

1. Alexander, J.I.D., Ouazzani, J., Rosenberger, F., 1989, Analysis of the low gravity tolerance of Bridgman-Stockbarger crystal growth: I. Steady and impulse accelerations, J. Crystal Growth, Vol. 97, pp. 285-302.
2. Alexander, J.I.D., Amiroudine S., Ouazzani, J., Rosenberger, F., 1991, Analysis of the low gravity tolerance of Bridgman-Stockbarger crystal growth: II. Transient and periodic accelerations, J. Crystal Growth, Vol. 113, pp. 21-38.
3. Garandet G.P., Corre S., Favier J.J. and Alexander, J.I.D, 1996, On the effect of gravity perturbations on composition profiles during Bridgman crystal growth in space, J. Crystal Growth, Vol. 165, pp. 471-481.
4. Voller, V.R., Brent, A.D. and Prakash, C., 1989, The modeling of heat, mass and solute transport in solidification systems, Int. J. Heat Mass Transfer, Vol. 32, pp 1719-1731.
5. Morgan, K., Lewis, R.W. and Zienkiewicz, O.C., 1978, An improved algorithm for heat conduction problems with phase change, Int. J. Numer. Meth. Eng., Vol.12, pp. 1191-1195.
6. Timchenko, V., Chen, P.Y.P., de Vahl Davis, G. and Leonardi, E., 1998, 'Directional Solidification in Microgravity', Heat Transfer 1998, J.S. Lee (ed), Taylor & Francis, pp. 241-246.

REPORT DOCUMENTATION PAGE

Form Approved
OMB No. 0704-0188

1. AGENCY USE ONLY (*Leave blank*)	2. REPORT DATE	3. REPORT TYPE AND DATES COVERED
	July 1999	Technical Memorandum

4. TITLE AND SUBTITLE

Effects of G-Jitter on Directional Solidification of a Binary Alloy

5. FUNDING NUMBERS

WU–963–35–0F–00

6. AUTHOR(S)

C. Benjapiyaporn, V. Timchenko, G. de Vahl Davis, E. Leonardi, and H.C. de Groh III

7. PERFORMING ORGANIZATION NAME(S) AND ADDRESS(ES)

National Aeronautics and Space Administration
John H. Glenn Research Center at Lewis Field
Cleveland, Ohio 44135–3191

8. PERFORMING ORGANIZATION REPORT NUMBER

E–11748

9. SPONSORING/MONITORING AGENCY NAME(S) AND ADDRESS(ES)

National Aeronautics and Space Administration
Washington, DC 20546–0001

10. SPONSORING/MONITORING AGENCY REPORT NUMBER

NASA TM—1999-209281
IAF–98–J.2.01

11. SUPPLEMENTARY NOTES

Prepared for the 49th International Astronautical Congress sponsored by the International Astronautical Federation, Melbourne, Australia, September 28—October 2, 1999. C. Benjapiyaporn, V. Timchenko, G. de Vahl Davis, and E. Leonardi, University of New South Wales, Syndey NSW, Australia; H.C. de Groh III, NASA Glenn Research Center. Responsible person, H.C. deGroh III, organization code 6712, (216) 433–5025.

12a. DISTRIBUTION/AVAILABILITY STATEMENT

Unclassified - Unlimited
Subject Categories: 29, 26 and 34 Distribution: Nonstandard

This publication is available from the NASA Center for AeroSpace Information, (301) 621–0390.

12b. DISTRIBUTION CODE

13. ABSTRACT (***Maximum 200 words***)

A study of directional solidification of a weak binary alloy (specifically, Bi - 1 at% Sn) based on the fixed grid single domain approach is being undertaken. The enthalpy method is used to solve for the temperature field over the computational domain including both the solid and liquid phases; latent heat evolution is treated with the aid of an effective specific heat coefficient. A source term accounting for the release of solute into the liquid during solidification has been incorporated into the solute transport equation. The vorticity-stream function formulation is used to describe thermo-solutal convection in the liquid region. In this paper we present a numerical simulation of g-jitter. A background gravity of 1 μg has been assumed, and new results for the effects of periodic disturbances over a range of amplitudes and frequencies on solute field and segregation have been presented.

14. SUBJECT TERMS	15. NUMBER OF PAGES
Gravity; Connection; Diffusion; Microgravity processing	16
	16. PRICE CODE: A03

17. SECURITY CLASSIFICATION OF REPORT	18. SECURITY CLASSIFICATION OF THIS PAGE	19. SECURITY CLASSIFICATION OF ABSTRACT	20. LIMITATION OF ABSTRACT
Unclassified	Unclassified	Unclassified	